Observation of Multiple Scattering in $(e, 2e)$ Experiments on Small Argon Clusters

Thomas Pflüger,* Arne Senftleben, Xueguang Ren, Alexander Dorn, and Joachim Ullrich

Max-Planck-Institut für Kernphysik, Saupfercheckweg 1, 69117 Heidelberg, Germany

(Received 27 June 2011; published 21 November 2011)

A kinematically complete experiment for 100 eV electron-impact ionization of small argon clusters was realized. The triple coincidence detection of both outgoing electrons and the residual ion allows the discrimination between single ionization of atoms, dimers and non-mass-selected small clusters as well as between ionization and excitation within the same cluster. Comparison of fully and partly differential ionization cross sections for clusters with those of atoms reveal clear signatures of multiple-scattering reactions. For ionization with excitation, an almost isotropic electron emission pattern is observed.

DOI: 10.1103/PhysRevLett.107.223201 PACS numbers: 34.80.Dp

Cluster studies allow us to observe the transition from atomic properties to bulklike behavior as a function of increasing cluster size. In the past decade noble gas clusters which show weak van der Waals binding have attracted considerable interest. Because of their small two-particle binding energies ranging from 10^{-7} eV for He_2 to 12 meV for Ar_2 and the resulting large internuclear distances, they often behave as if each atom is nearly independent. These systems allow us to investigate a number of new phenomena which emerge if an atom is embedded into an environment and which are absent for isolated atoms. In recent years, in particular, the response to electronic excitation of atoms within small noble gas clusters has been intensely studied. This interest was initiated by the theoretical prediction that relaxation via electron emission can result from energy or electron exchange between neighboring sites [1] resulting in the interatomic Coulombic decay (ICD) and the electron transfer mediated decay [2], respectively. More recently, theory found strongly enhanced direct photoionization through resonant energy transfer between atoms [3] as well as the modification of Auger decay within a charged cluster environment [4]; other recent studies include ion collisions [5] and interactions with intense laser pulses [6,7].

In the present study we demonstrate that the multicenter structure of small noble gas clusters modifies the fundamental few-body dynamics in electron-impact ionization of atoms leading to additional scattering. The observation of the ionized electron emission pattern over a large part of the full solid angle sheds new light on a recent hot debate initiated by Schulz *et al.* [8] concerning the influence of higher-order or multiple-scattering processes on the (emission pattern) cross section shape.

For a single-interaction binarylike knockout of an atomic target, electron emission into the projectile scattering plane is favored. In contrast, for fast ion impact Schulz *et al.* have found substantial electron emission in the direction perpendicular to the scattering plane which up to the present day could not be reproduced by theory. Possible mechanisms which are under discussion include multiple scattering of the projectile, a nonadequate description of the target potential by theory [9,10] or, most recently, incoherent scattering processes [11].

Moreover, a number of studies aim to clarify the role of multiscattering reactions by proceeding to more heavy atoms such as magnesium or argon. Because of their increased nuclear charge, stronger nuclear scattering [12] is expected. Finally, comparative studies on targets having an equal number of electrons but different nuclear structure such as atomic helium and molecular H_2 have been reported to tackle this question [13]. Unfortunately, the interpretation is not straightforward since the change of target structure is always accompanied by the modification of several other parameters such as the electronic wave functions and binding energies.

In order to overcome these restrictions we use small noble gas clusters as a target. Compared to atoms, the electronic wave functions of the individual scattering centers are only slightly modified and the comparison of the cross section for atoms and clusters of different size can give direct information on the influence of additional multiple-scattering effects. So far $(e, 2e)$ studies on clusters have not been feasible due to the dilute nature of cluster sources and the low efficiency of standard $(e, 2e)$ coincidence techniques. Here, we present for 100 eV electron-impact energy fully, triple-differential cross sections (3DCSs) for Ar atoms, Ar_2 dimers and partial integrated cross sections, summed over all masses for Ar_n $(n > 2)$.

The experiments are enabled, on one hand, by a target produced by supersonic expansion of argon gas delivering a collimated internally cold (1 K) gas jet. It contains a 2% fraction of dimers and 1% of heavier clusters with a mean cluster size of $\langle n \rangle \sim 25$ at the present experimental conditions [14]. The low particle number density is compensated for, on the other hand, by using a highly efficient reaction microscope [15–17] covering a relatively large phase space. Its basic principle is the extraction of the ion and both electrons by means of homogeneous electric and magnetic fields into opposite directions and their projection onto two position sensitive detectors. Since

position and time information for each fragment is recorded their complete momentum vectors can be extracted.

The momenta of the two outgoing electrons define the collision kinematics and the energy deposition (the Q value) of the reaction. The recoiling ion provides information on the target species. Collisions involving Ar and Ar_2 can be distinguished by the mass-to-charge ratio of the respective ion. The small clusters, on the other hand, show strong fragmentation after ionization due to the formation of a vibrationally highly excited dimer ion within the cluster. The vibrational energy amounts up to 1.2 eV and is released by evaporating essentially all other neutral atoms [18] such that the dimer ion Ar_2^+ is by far the most abundant product [19]. Nevertheless, collisions involving dimers and small clusters can be distinguished in terms of the resulting Ar_2^+ recoil momentum. For the pure ionization of Ar_2 the resulting Ar_2^+ ion momentum is rather small (< 0.6 a.u.). In contrast, dimer ions resulting from the fragmentation of small clusters obtain significantly larger momenta (up to 15 a.u.) due to the dissociative nature of the process.

Figure 1 shows the binding energy spectra for the different target species investigated. We define the binding energy $E_{\text{bind.}}$ as the initial projectile energy minus the sum energy of the two final state electrons [i.e., $E_{\text{bind.}} = E_{e0} - (E_{e1} + E_{e2})$]. The instrumental linewidth is about 10 eV which is consistent with a momentum resolution of 0.1 a.u. for both outgoing electrons. For all targets one can see a dominant peak at around 16 eV which corresponds to pure ionization of the outer $3p$ electron in atomic argon. The atomic case exhibits an additional feature at 35 eV which we attribute to simultaneous ionization and excitation to the $Ar^{+*}(3p^{-1}nl)$ states. This assignment is in accordance with the absence of this feature for the Ar_2 target with Ar_2^+ ion detection: above $E_{\text{bind.}} = 29$ eV the Ar_2^{+*} ion is not stable but dissociates [20]. Above $E_{\text{bind.}} = 35$ eV ICD is enabled where the dimer fragments

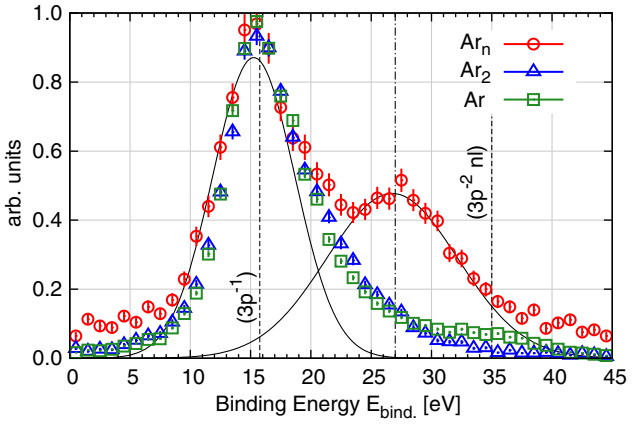

FIG. 1 (color online). Binding energy spectrum for the ionization of atomic argon and argon dimers and small argon clusters. The dashed line marked $(3p^{-1})$ indicates the first ionization potential of atomic argon. The Gaussians are fitted to the Ar_n data.

efficiently into two Ar^+ ions. Finally, for small clusters Ar_n ($n > 2$) a second prominent peak is located at 27 eV, i.e., about 12 eV above the main peak. This energy is consistent with a double scattering reaction where in addition to ionization of one cluster atom a second Ar atom is excited, e.g., to the lowest excited configuration $3p^5 4s$, 11.6 eV above the ground state. Strictly speaking an excitonic state is formed [21].

Experimental 3DCSs for 100 eV electron-impact ionization of Ar atoms and Ar_2 dimers are shown in Fig. 2 for particular kinematical parameters. The emission angle and energy of the scattered electron e_1 are fixed to $\theta_{e1} = 15°$ and $E_{e1} = 74$ eV, respectively, resulting in an angle of the momentum transfer $\vec{q}$ of 53° as indicated in Fig. 2(b). Each data set was normalized to its respective 4π cross section for this particular kinematical condition. The ejected electron energy $E_{e2} = 10$ eV was chosen such, that the total cross section σ_E for elastic scattering at a neighboring atom is maximal ($\sigma_E = 2 \times 10^{-15}$ cm^2) [22]. For example, already for the dimer with a mean internuclear distance of 3.8 Å a rescattering probability of 11% is obtained, while only 1.7% would be expected on the basis of solely geometrical considerations. In Fig. 2(b) the 3DCS for ejection into the projectile scattering plane is plotted as a function of the emission angle θ_{e2} of e_2. This plane contains the dominant features of the cross section due to first order processes. The so-called binary peak is roughly aligned along q for ejection of the target electron in a binary collision and the recoil lobe in the opposite direction due to backscattering of the ejected electron in the ionic potential. For atomic argon a state-of-the-art distorted-wave R-matrix calculation (DWB2-RM) is presented [23,24] which has proven to be a rather good description at impact energies larger 200 eV [12]. Here, at lower energy it can only be expected to be in qualitative agreement since, e.g., the long range Coulomb repulsion of both final state electrons is not considered (so-called post-collision interaction, PCI). This gives rise to the overestimation of the 3DCS in the forward direction ($\theta_{e2} = 0° \pm 50°$) and to the angular shifts of the experimental peaks away from the emission angle of e_1 towards the backwards direction. These shifts can also contribute to the filling up of the minimum around $\theta_{e2} = 180°$ in the experimental data. In the past multiple-scattering effects involving the nucleus were also discussed to give rise to similar effects [12].

All data sets for atoms and dimers are normalized relative to each other to the respective integral counts over the complete 4π solid angle of the ejected electrons for this particular kinematical condition (i.e., $\theta_{e1} = 15°$, $E_{e1} = 74$ eV). This procedure assumes that the presence of the neighboring atom in the dimer does not change the single-ionization cross section. While the general behavior of both 3DCSs is similar, distinct differences are observed. First, the binary peak maximum shows a slight forward shift by about 10° to 15° and second, the cross section in the region

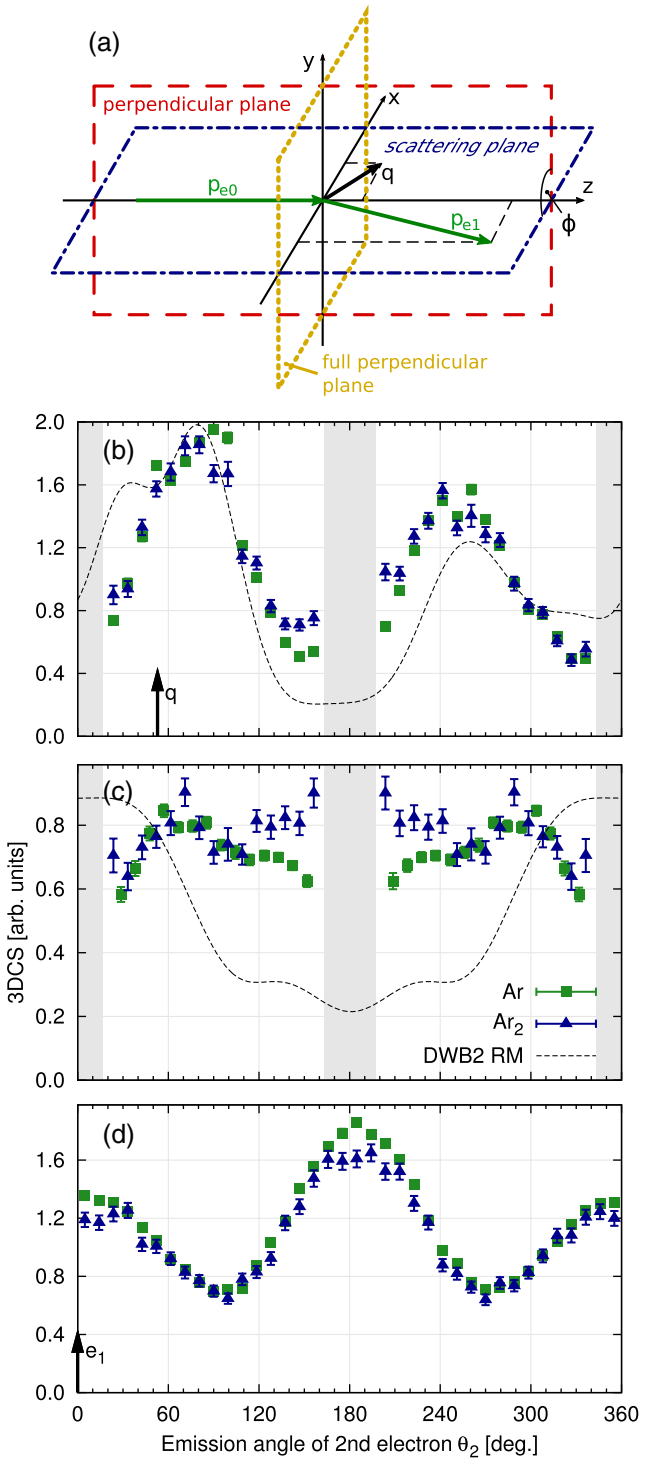

FIG. 2 (color online). (a) Scattering geometry. The momentum transfer is denoted by q. The scattering plane is defined by $\phi = 0°$, the perpendicular plane by $\phi = 90°$. The full perpendicular plane is orthogonal to the projectile momentum vector p_0. (b) 3DCS for $(e, 2e)$ on argon dimers (▲) and atomic argon (■) in the scattering plane, (c) the perpendicular plane and (d) full perpendicular plane. The scattering angle is $\theta_{e1} = -15°$ and the ejection energy $E_{e2} = 10$ eV. The dashed line represents a hybrid distorted-wave R-matrix calculation for atomic argon [24]. Data are normalized to the respective integral over the ejected electron 4π solid angle.

around $\theta_{e2} = 180°$ is increased. A tentative explanation of the angular shift is reduced PCI due to shielding by the second atom while the filling of the backwards minimum is consistent with additional scattering. This last point becomes more obvious in Fig. 2(c). Here electron emission in the perpendicular plane is plotted which is rotated with respect to the scattering plane by $\phi = 90°$ around the incoming beam axis as illustrated in panel 2(a). Since the cross section in this observation plane is not dominated by the binary and recoil peaks it is more sensitive to higher-order effects. Indeed, the dimer cross section is increased in the complete backwards hemisphere, clearly demonstrating the enhanced sensitivity to the cross section on multiple-scattering effects in this plane. Finally, panel 2(d) shows the full perpendicular plane with two peaks at 0° and 180° due to the binary and recoil peak, respectively. For dimers both peaks are reduced, e.g., due to redistribution of intensity to other directions.

Proceeding further in complexity, we studied collisions on small clusters where pure ionization could be distinguished from ionization with excitation of a second cluster atom. Because of strongly reduced number density for the small clusters and the resulting low count rates, the data were integrated over a range of scattering angles from $\theta_{e1} = -4°$ to $-20°$ and the ejection energies from $E_{e2} = 1.5$ eV to 20 eV.

For a qualitative comparison 3D emission patterns are presented in Fig. 3, for atomic argon 3(a), pure ionization of small clusters 3(b), and ionization plus excitation of small clusters 3(c). In all plots the projectile comes in from the bottom with a momentum labeled p_0 while the direction of the momentum transfer is indicated by the arrow labeled q. Compared to the atomic cross section, ionization of clusters depicts a modified binary peak shape as well as filling of the minimum separating the binary from the recoil lobe. For ionization and excitation the distribution looks almost perfectly isotropic.

A more quantitative comparison is possible for cuts through the 3D cross sections along all planes depicted in Fig. 2(a). In Fig. 4(a) the differential data for the scattering plane are shown. Like for the dimer data in Fig. 2, the ionization results for small argon clusters show filling of the 180° cross section minimum as well as around 340°,

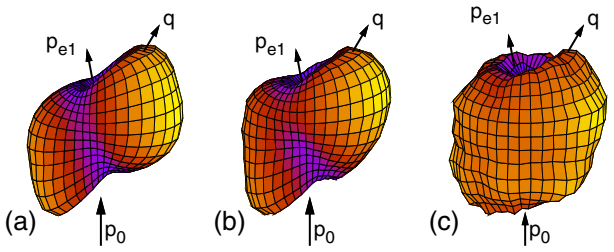

FIG. 3 (color online). 3D cross sections for pure ionization of (a) argon atoms, (b) small clusters and for additional excitation in (c) small clusters with the same kinematics as shown in Fig. 4.

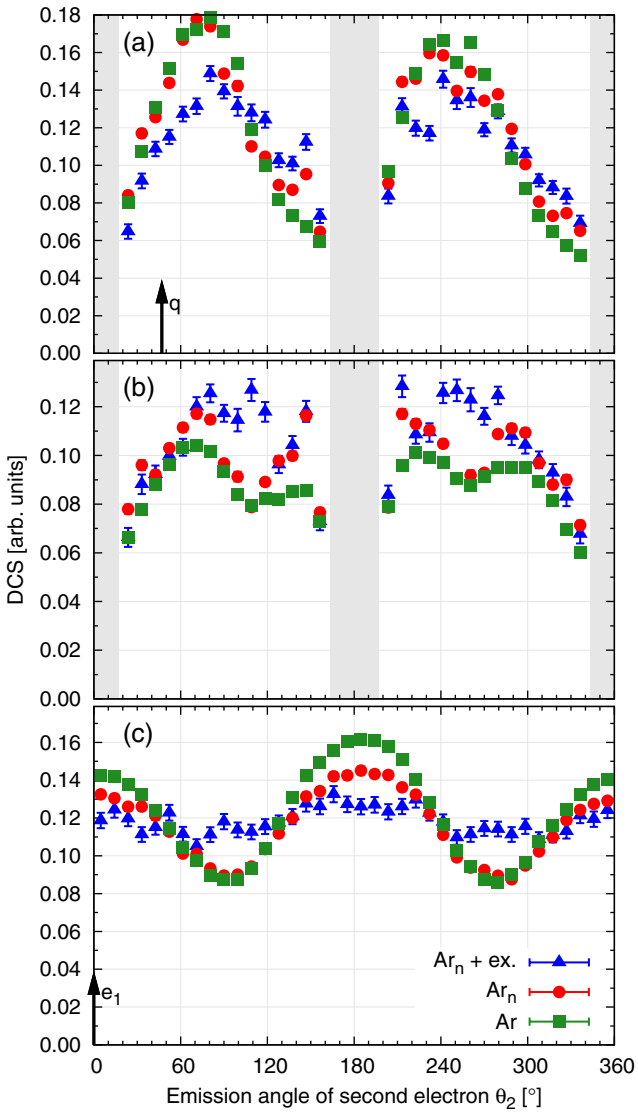

FIG. 4 (color online). Combined differential cross section for (a) the scattering plane, (b) perpendicular plane, and (c) the full perpendicular plane. The scattering angle of the first electron was $\theta_{e1} = -4°$ to $-20°$ while the ejection energy of the second electron was $E_{e2} = 1.5$ eV to 20 eV. Shown are the angular distributions of the ejected electrons for the pure ionization channel of the atom (■), of small clusters (●), and additional excitation in small clusters (▲). Gray shaded areas: no experimental acceptance. The normalization procedure is identical to what was applied in Fig. 2.

where in the atomic case suppression due to PCI is strong. For ionization with excitation, on the other hand, the angular shift of the peak positions is reversed with the binary peak positioned almost perfectly at 90°. This is pointing to complete randomization of the ejected electron direction due to multiple scattering. As a result, the cross section in the perpendicular plane in Fig. 4(b) rises significantly and structures as the minimum present at 110° for the monomer and for pure ionization of the cluster disappear completely. An even stronger effect can be seen in the full perpendicular plane [i.e., Fig. 4(c)] which cuts through the binary and recoil lobes resulting in maxima at $\theta_{e2} = 180°$ and 0°, respectively. For pure ionization, only a small decrease of the maxima with respect to the atomic case is visible, while the minima at 90° and 270° persist. For simultaneous ionization plus excitation the minima are filled resulting in an almost isotropic distribution. Interestingly our results for pure ionization are not in agreement with the interpretation of the above mentioned strong out-of-plane emission observed for particle impact ionization of atoms and molecules [8,12]. Just perpendicular to the scattering plane, i.e., for angles $\theta_{e2} = 90°$ and 270° in Figs. 2(c), 4(b), and 4(c), the cross section for dimers and clusters is essentially identical to the atomic one. On the other hand, for simultaneous ionization plus excitation where each reaction definitely involves two-center scattering, strongly increased perpendicular plane emission is present. Therefore, the influence of the cluster environment on the pure ionization must be more subtle than just additional elastic scattering. A detailed theoretical treatment including, e.g., explicit molecular electronic wave functions would be highly desirable.

To summarize, the first kinematically complete $(e, 2e)$ experiments on argon dimers and small argon clusters have been performed. Triple-differential cross sections for the $3p$ ionization of Ar_2 where presented and compared to those of atomic argon. Here, we found increased emission of ejected electrons in the backward direction as well as an overall enhancement in the cross section for out-of-plane emission. Moreover, 3D differential cross sections for the electron-impact ionization of small argon clusters with a mean size of 25 atoms/cluster were obtained. Two main reaction channels have been observed and are assigned to pure ionization and simultaneous ionization plus excitation of two different cluster constituents, respectively. Significant differences in cross section shape were found compared to those for atomic argon. These differences can be attributed to the redistribution of emission angles due to additional elastic and inelastic scattering and possibly to less pronounced post-collision interaction. In addition the presence of a neighboring ion could modify elastic scattering at a neutral atom. These observations emphasize the particular importance of out-of-plane investigations. So far no theoretical calculations obtaining 3DCSs for electron-impact ionization of clusters are available.

We thank Klaus Bartschat for suppling theoretical data in numerical form. X. R. is grateful for support from DFG Project No. RE 2966/1-1.

*thomas.pflueger@mpi-hd.mpg.de

[1] L. S. Cederbaum, J. Zobeley, and F. Tarantelli, Phys. Rev. Lett. **79**, 4778 (1997).

[2] J. Zobeley, R. Santra, and L. S. Cederbaum, J. Chem. Phys. **115**, 5076 (2001).

[3] B. Najjari, A. B. Voitkiv, and C. Müller, Phys. Rev. Lett. **105**, 153002 (2010).
[4] V. Averbukh, U. Saalmann, and J. M. Rost, Phys. Rev. Lett. **104**, 233002 (2010).
[5] J. Matsumoto *et al.*, Phys. Rev. Lett. **105**, 263202 (2010).
[6] B. Ulrich *et al.*, Phys. Rev. A **82**, 013412 (2010).
[7] B. Manschwetus *et al.*, Phys. Rev. A **82**, 013413 (2010).
[8] M. Schulz *et al.*, Nature (London) **422**, 48 (2003).
[9] D. H. Madison *et al.*, Phys. Rev. Lett. **91**, 253201 (2003).
[10] M. Foster *et al.*, Phys. Rev. Lett. **97**, 093202 (2006).
[11] K. N. Egodapitiya *et al.*, Phys. Rev. Lett. **106**, 153202 (2011).
[12] X. Ren *et al.*, J. Phys. B **43**, 035202 (2010).
[13] O. Al-Hagan, C. Kaiser, D. Madison, and A. J. Murray, Nature Phys. **5**, 59 (2009).
[14] O. F. Hagena, Surf. Sci. **106**, 101 (1981).
[15] J. Ullrich *et al.*, Rep. Prog. Phys. **66**, 1463 (2003).
[16] M. Dürr *et al.*, Phys. Rev. Lett. **98**, 193201 (2007).
[17] A. Dorn *et al.*, J. Electron Spectrosc. Relat. Phenom. **161**, 2 (2007).
[18] D. Bonhommeau, N. Halberstadt, and A. Viel, J. Chem. Phys. **124**, 184314 (2006).
[19] J. M. Soler, J. J. Saenz, N. Garcia, and O. Echt, Chem. Phys. Lett. **109**, 71 (1984).
[20] P. Lablanquie *et al.*, J. Chem. Phys. **127**, 154323 (2007).
[21] U. Hergenhahn *et al.*, Chem. Phys. Lett. **351**, 235 (2002).
[22] B. Mielewska, I. Linert, G. C. King, and M. Zubek, Phys. Rev. A **69**, 062716 (2004).
[23] K. Bartschat and P. G. Burke, J. Phys. B **20**, 3191 (1987).
[24] K. Bartschat (private communication).